# In-out asymmetry of surface excitations in reflection-electron-energy-loss spectra of polycrystalline Al

Francesc Salvat-Pujol
*Institut für Theoretische Physik, Goethe-Universität Frankfurt, Max-von-Laue-Straße 1, 60438 Frankfurt am Main, Germany*

Wolfgang S. M. Werner
*Institut für Angewandte Physik, Technische Universität Wien, Wiedner Hauptstraße 8-10/134, 1040 Vienna, Austria*

Mihaly Novák
*Institute of Nuclear Research of the Hungarian Academy of Sciences, MTA ATOMKI, 18/c Bem tér, H-4026 Debrecen, Hungary*

Petr Jiricek and Josef Zemek
*Institute of Physics, Academy of Sciences of the Czech Republic, Na Slovance 2, 182 21 Prague 8, Czech Republic*
(Received 11 December 2013; revised manuscript received 30 April 2014; published 28 May 2014)

We present experimental evidence for differences in surface energy losses between (a) electrons entering a solid from vacuum and (b) electrons leaving the solid into vacuum. Although these so-called in-out asymmetries have been long assumed to exist on theoretical grounds, the present work constitutes a clear experimental observation of the phenomenon. The effect has been exposed by comparing reflection-electron-energy-loss spectra of polycrystalline Al for pairs of conjugate scattering geometries where the directions of the source and the detector were interchanged. Differences of up to 30% in the peak height of surface energy-loss features are observed. The experimentally observed in-out asymmetry has been examined within the semiclassical dielectric formalism using state-of-the-art models for surface scattering of charged projectiles. The theoretical analysis suggests that in-out asymmetry effects are most accentuated for surface-crossing directions close to the surface normal and for high kinetic energies, in good agreement with the observed behavior. The effect is assumed to be present not only for electrons, but in principle for any charged particle.

DOI: 10.1103/PhysRevB.89.205435 PACS number(s): 68.49.Jk, 79.20.Uv, 82.80.Pv

## I. INTRODUCTION

With the advent of increasingly surface-sensitive techniques such as near-field-emission scanning electron microscopy [1,2] and the widespread use of electron beams in nanotechnology [3,4], detailed knowledge of fine-grained details of the electrodynamics of charged projectiles near solid surfaces is of increasing relevance, both from an applied and from a fundamental point of view. In particular, a sound understanding of the energy-loss process of incoming projectiles near the surface is instrumental not only for quantitative purposes in spectroscopy applications, but also in better characterizing, e.g., growth conditions in electron-beam-induced deposition of nanostructures and post-growth treatments with electron beams [5,6]. In the present work we address the differences in the energy-losses of charged projectiles crossing a solid surface (1) from vacuum into the solid and (2) from the solid into vacuum. Theoretical accounts of the electronic stopping of charged projectiles near planar interfaces often suggest in passing that these in-out asymmetries exist [7–10]; very recently, an article has been published [11] where in-out asymmetries in perpendicular surface crossings were discussed on the basis of the semiclassical dielectric formalism with a simplified single-pole dielectric function. In spite of the acknowledged existence of the in-out-asymmetry effect on theoretical grounds and of its longstanding history in theoretical discussions, no direct experimental observation of this asymmetry has been reported to date. Furthermore, no detailed examination of the behavior of the effect as a function of the projectile's kinetic energy and surface-crossing angle has been performed. State-of-the-art models of electron transport through planar interfaces [8,10,12,13] include this phenomenon and thus provide a valuable tool for finding convenient scattering geometries to expose it experimentally. In this article we examine the in-out asymmetry on the basis of the semiclassical dielectric formalism, we discuss its qualitative behavior as a function of the electron kinetic energy and the surface-crossing angle, and we present a series of experimental electron-energy-loss spectra, which clearly exhibit the asymmetry, in good agreement with the behavior expected from our theoretical analysis. The presented data constitute a clear experimental evidence for the existence of the effect.

It should be noted that exposing the in-out-asymmetry of surface excitations experimentally is far from trivial. On the one hand, because electrons can only be detected outside of the solid, the experimental possibilities are restricted to either reflection or transmission electron-energy-loss experiments. Discriminating between incoming and outgoing trajectories is possible in a reflection geometry by comparing reflection-electron-energy-loss (REEL) spectra recorded for two conjugate scattering geometries, where the direction of the source and the detector are interchanged [14]. Such an operation is not possible in conventional transmission experiments, which is why transmission experiments are discarded for the present purposes. On the other hand, as we show below, the in-out asymmetry is expected to be weak for oblique surface-crossing angles. Thus, comparing (a) REEL spectra for a scattering geometry having an oblique incidence direction and a perpendicular detection direction with (b) REEL spectra for

 

the conjugate geometry should result in a net observable effect due to the asymmetry in the *perpendicular* surface-crossing segments (see first paragraph of Sec. III). Furthermore, since the in-out asymmetry in surface excitations is predicted to be an overall subtle effect, it is convenient to choose a material that exhibits well-separated surface and bulk energy-loss features, such as Al, in order to avoid the use of multiple-scattering deconvolution procedures, which might introduce additional uncertainties in the results. For such materials as Al, the effect should be visible in the raw REEL data with the bare eye. For these reasons, we used REEL measurements of an Al sample to expose the in-out asymmetry in surface excitations.

## II. THEORY

A detailed account of the stopping of nonrelativistic charged projectiles in the vicinity of a planar solid interface has been recently published [10,15], based on the semiclassical dielectric formalism. Within this formalism, the agent responsible for the stopping of the projectile is the induced electric field due to the polarization of the solid in response to the presence of the swift charged projectile. This induced electric field arises from a bulk polarization charge, which yields the well-known bulk-stopping characteristics, and a surface polarization charge, which on the one hand suppresses bulk energy-loss modes (Begrenzung effect) and on the other hand activates surface-excitation modes.

In this section we analyze the stopping power (average energy loss per unit path length) of a charged projectile in the immediate vicinity of a planar surface for different kinetic energies and surface-crossing angles, focusing on asymmetries between incoming and outgoing trajectories. We base our discussion on the stopping power due to the fact that it is at present difficult to obtain a combination of (a) a dielectric-function model and (b) a surface-excitation model that simultaneously yields a good position and width of the surface-plasmon peak for Al [16]. We therefore restrict our theoretical considerations to a qualitative description of the observed phenomenon on the basis of an integrated quantity.

The geometry of the problem is depicted in Fig. 1. A system of Cartesian coordinates is oriented so that the surface of the medium is the plane $z = 0$ and the positive $z$ axis points toward the vacuum. The $x$ and $y$ axes are oriented so that the trajectory of the projectile lies in the plane $y = 0$.

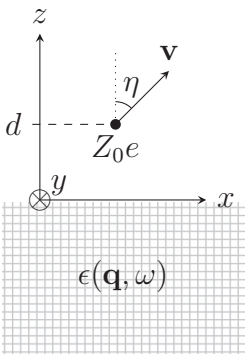


FIG. 1. Geometry of the transport problem in the vicinity of a solid surface.

A projectile of charge $Z_0 e$ moves with a velocity $\mathbf{v}$ (with a corresponding kinetic energy $E$ with respect to the Fermi level) forming an angle $\eta$ with the surface normal. Notice that $\eta < 90^\circ$ corresponds to outgoing trajectories, whereas $\eta > 90^\circ$ corresponds to incoming trajectories. The $z$ coordinate of the position of the projectile with respect to the surface at a time $t$ is given by $d = v_z t$. Thus, the projectile crosses the interface at $t = 0$. The variable $d$ is used instead of $z$ to retain consistency with Ref. [10]. Note that $d > 0$ indicates the vacuum side of the surface and $d < 0$ indicates the Al side of the surface. Furthermore, regardless of the value of $\eta$, for $t < 0$ the projectile has yet to cross the surface, whereas for $t > 0$ the projectile has left the interface behind.

Within the semiclassical model for surface excitations presented in Ref. [10], the stopping power $S$ of the charged projectile in a homogeneous medium is given by

$$S = \frac{\mathrm{i}}{\pi}\frac{Z_0}{v}\int_{-\infty}^{\infty} d\omega\,\omega \int_{\mathbb{R}^3} d\mathbf{q}\, e^{\mathrm{i}t(\mathbf{q}\cdot\mathbf{v}-\omega)}\frac{1}{q^2} \times \left\{\frac{Z_0}{2\pi}\delta(\omega-\mathbf{q}\cdot\mathbf{v})\left[\frac{1}{\epsilon(\mathbf{q},\omega)}-1\right] + \rho_s(\mathbf{q}_\parallel,\omega)\left[\Theta(d)-\frac{\Theta(-d)}{\epsilon(\mathbf{q},\omega)}\right]\right\}, \quad (1)$$

where atomic units ($\hbar = m_e = e = 1$) are used and where $\Theta(d)$ is the Heaviside step function (1 if $d > 0$ and 0 if $d < 0$), $\epsilon(\mathbf{q},\omega)$ is the wavevector ($\mathbf{q}$) and frequency ($\omega$) dependent dielectric function of the medium, and $\rho_s(\mathbf{q}_\parallel,\omega)$ is the Fourier transform of the induced surface charge, discussed below. Using the property $\epsilon(-\mathbf{q},-\omega) = \epsilon^*(\mathbf{q},\omega)$ we have

$$S = -\frac{2}{\pi}\frac{Z_0}{v}\int_0^{\infty} d\omega\,\omega \int_{\mathbb{R}^3} d\mathbf{q}\,\frac{1}{q^2}\mathrm{Im} \times \left\{e^{\mathrm{i}t(\mathbf{q}\cdot\mathbf{v}-\omega)}\frac{Z_0}{2\pi}\delta(\omega-\mathbf{q}\cdot\mathbf{v})\left[\frac{1}{\epsilon(\mathbf{q},\omega)}-1\right] + e^{\mathrm{i}t(\mathbf{q}\cdot\mathbf{v}-\omega)}\rho_s(\mathbf{q}_\parallel,\omega)\left[\Theta(d)-\frac{\Theta(-d)}{\epsilon(\mathbf{q},\omega)}\right]\right\}. \quad (2)$$

The semiclassical approximation consists in identifying $\hbar\mathbf{q}$ as the momentum transfer from the projectile to the medium and $\hbar\omega$ as the energy loss of the projectile. This implies that the integrals should now be restricted to the kinematically allowed domain: the integral over $\omega$ should be restricted to the domain $[0,E]$ and the integral over $\mathbf{q}$ should be restricted to $q = |\mathbf{q}| \in [q_-,q_+]$, where, for electrons,

$$q_\pm = \sqrt{2E} \pm \sqrt{2(E-\omega)}. \quad (3)$$

We furthermore make the assumption that the dielectric function depends on the wavevector $\mathbf{q}$ only through its modulus, that is, $\epsilon(\mathbf{q},\omega) = \epsilon(q,\omega)$. The first term in the braces of Eq. (2) then yields

$$S_B = -\frac{2}{\pi}\frac{Z_0^2}{v^2}\int_0^{E} d\omega\,\omega\int_{q_-}^{q_+} dq\,\frac{1}{q}\mathrm{Im}\left[\frac{1}{\epsilon(q,\omega)}\right], \quad (4)$$

the well-known expression for the stopping of a charged projectile in a bulk medium.

The second term of Eq. (2) gives the contribution to the stopping power due to the excitation of surface modes,

$$S_S = -\frac{2}{\pi}\frac{Z_0}{v}\int_0^\infty d\omega\,\omega\int_{\mathbb{R}^3} d\mathbf{q}\,\frac{1}{q^2}\mathrm{Im} \times\left\{e^{i\tau(\mathbf{q}\cdot\mathbf{v}-\omega)}\rho_s(\mathbf{q}_\parallel,\omega)\left[\Theta(d)-\frac{\Theta(-d)}{\epsilon(\mathbf{q},\omega)}\right]\right\}.$$

Within the present model, the induced surface charge reads [10]

$$\rho_s(\mathbf{q}_\parallel,\omega) = \frac{Z_0}{2\pi}\frac{|v_z|}{q_\parallel^2 v_z^2+(\omega-\mathbf{q}_\parallel\cdot\mathbf{v}_\parallel)^2} \times\frac{\frac{1}{\epsilon(\mathbf{q}_\parallel,\omega)}-1}{\int_{-\infty}^{\infty}dk_z\,\frac{1}{q_\parallel^2+k_z^2}\left[1+\frac{1}{\epsilon(\mathbf{q}_\parallel,k_z,\omega)}\right]}. \quad (5)$$

The integral in the denominator can be simplified by assuming that $\epsilon(\mathbf{q},\omega)\approx\epsilon(\mathbf{q}_\parallel,\omega)$. This implies that the term in square brackets in the denominator can be pulled out of the integral and the remaining integral can be calculated analytically:

$$\int_{-\infty}^{\infty}dk_z\,\frac{1}{q_\parallel^2+k_z^2}=\frac{\pi}{q_\parallel}. \quad (6)$$

This approximation, carried out at this instance and at no other point in the calculation, has been shown [10] to shift the frequency and intensity of surface energy-loss modes, but nevertheless still captures a realistic energy- and angular-dependence of all surface characteristics. Thus, we have

$$\rho_s(\mathbf{q}_\parallel,\omega)=\frac{Z_0}{2\pi^2}\frac{q_\parallel|v_z|}{q_\parallel^2 v_z^2+(\omega-\mathbf{q}_\parallel\cdot\mathbf{v}_\parallel)^2}\frac{1-\epsilon(\mathbf{q}_\parallel,\omega)}{1+\epsilon(\mathbf{q}_\parallel,\omega)}, \quad (7)$$

and, therefore, with the semiclassical approximation we can write

$$S_S = -\frac{1}{\pi^3}Z_0^2\frac{|v_z|}{v}\int_0^E d\omega\,\omega\int_{q_-}^{q_+}e^{-q_\parallel|d|}q_\parallel \times\int_0^\pi d\theta\,\sin\theta\int_0^{2\pi}d\varphi\,\frac{1}{q_\parallel^2 v_z^2+(\omega-q_\parallel v_x\cos\varphi)^2} \times\mathrm{Im}\left\{e^{i\tau(q_\parallel v_x\cos\varphi-\omega)}\left[\Theta(d)-\frac{\Theta(-d)}{\epsilon(q,\omega)}\right]\frac{1-\epsilon(q_\parallel,\omega)}{1+\epsilon(q_\parallel,\omega)}\right\}. \quad (8)$$

In our calculations we have used the following simple oscillator model for the inverse dielectric function:

$$\frac{1}{\epsilon(q,\omega)}=1-\frac{\Omega_p^2}{Z_1}\sum_{j=1}^{n}\frac{f_j}{w_j^2+\frac{q^4}{4}-\omega^2-i\gamma_j\omega}, \quad (9)$$

where

$$\Omega_p=\sqrt{4\pi\mathcal{N}Z_1} \quad (10)$$

is the plasma frequency of a free electron gas with $\mathcal{N}Z_1$ electrons per unit volume, $Z_1$ is the atomic number of the material, and $\omega_j$ (eV), $\gamma_j$ (eV), and $f_j$ (dimensionless) are the frequency, damping parameter, and amplitude of the $j$th oscillator, respectively. To model Al ($Z_1=13$) we have used, as a first approximation, a single oscillator with $\omega_1=15$ eV, $\gamma_1=1.5$ eV, $f_j=3$, and $\Omega_p=32.84$ eV.

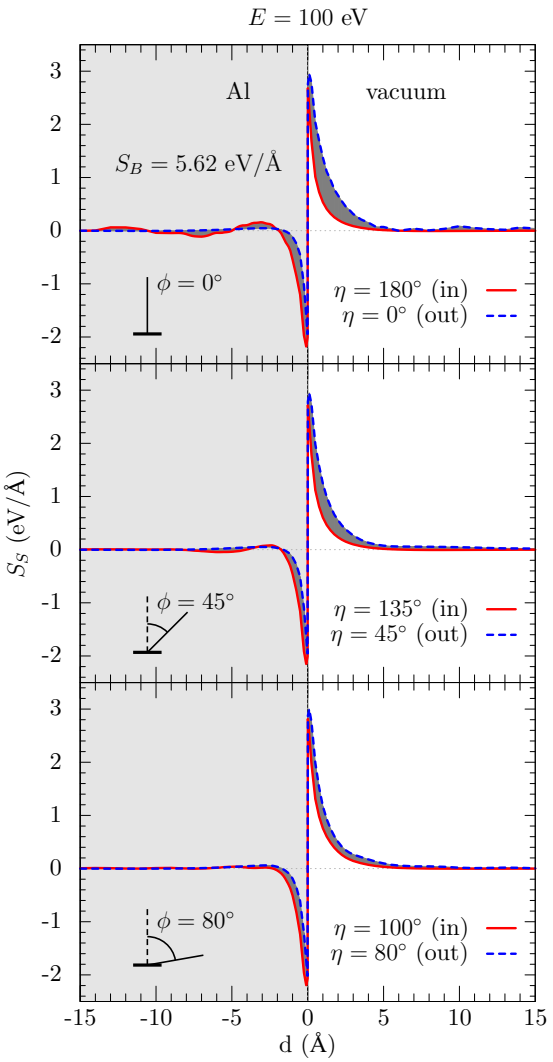


FIG. 2. (Color online) Contribution to the stopping power due to surface excitations, $S_S$ [Eq. (8)], of a 100-eV electron penetrating an Al surface from vacuum (solid red curves) and leaving the Al surface into vacuum (dashed blue curves) with an inclination of $\phi=0°$ (upper panel), 45° (middle panel), and 80° (lower panel) with respect to the surface normal. The negative excursion in the Al side of the interface corresponds to the suppression of bulk modes (Begrenzung effect). The total stopping power, $S_S+S_B$, remains a positive quantity.

Figure 2 displays the surface contribution to the stopping power, Eq. (8), as a function of the $z$ coordinate of the trajectory in the immediate vicinity of the interface (from $-15$ Å to $+15$ Å) for a 100-eV electron traversing the interface from vacuum into Al (red solid line, incoming) and from Al into vacuum (blue dashed line, outgoing) for trajectories with an inclination $\phi=0°$ (top panel), 45° (middle panel), and 80° (lower panel) with respect to the surface normal; the actual surface-crossing angle $\eta$ for the incoming and for the outgoing trajectory is indicated in Fig. 2. A label in the upper panel indicates the value of the bulk stopping power $S_B$ in the material, Eq. (4). In the Al side of the interface ($d<0$), indicated by a light-gray shade in Fig. 2, the negative contribution of the surface stopping power corresponds to the

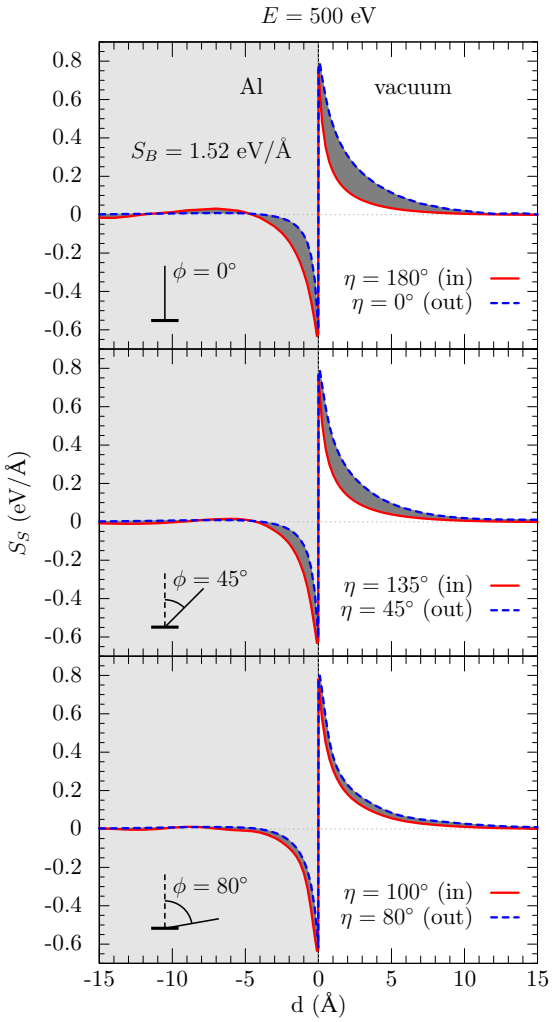


FIG. 3. (Color online) Same as described in the legend of Fig. 2 for $E = 500$ eV.

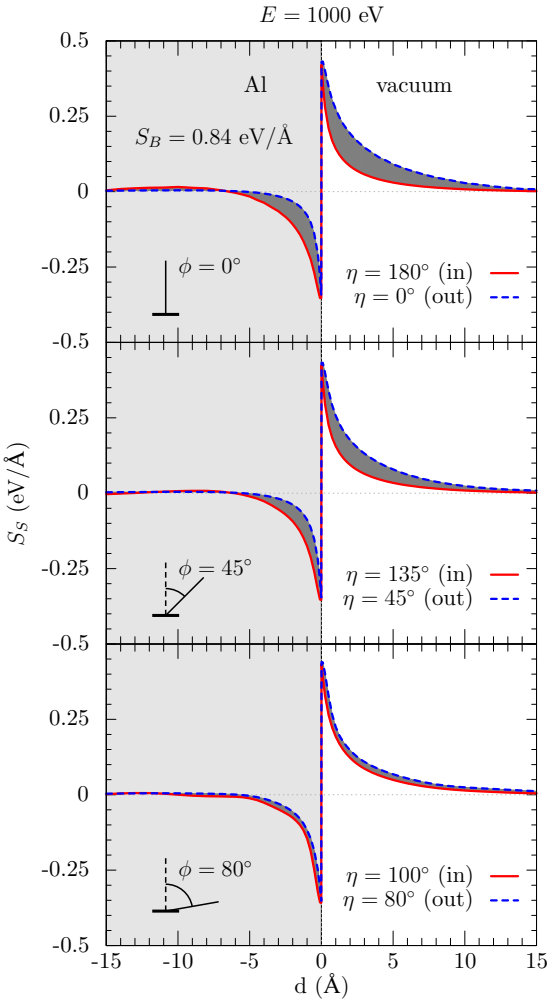


FIG. 4. (Color online) Same as described in the legend of Fig. 2 for $E = 1000$ eV.

Begrenzung effect, i.e., to the suppression of bulk modes. The total stopping power, $S_S + S_B$, remains a positive quantity. At the vacuum side of the interface ($d > 0$) energy losses are due to the excitation of surface modes only. We see that incoming and outgoing trajectories indeed exhibit noticeable differences. The area between the two curves is shaded in dark gray in order to aid the eye in quickly assessing the magnitude of differences in the stopping characteristics between incoming and outgoing trajectories, i.e., the magnitude of the in-out asymmetry. We find that in-out asymmetries are appreciable for perpendicular surface crossings (upper panel of Fig. 2), gradually diminish for increasing surface-crossing angles with respect to the surface normal (middle panel of Fig. 2), and finally vanish for grazing trajectories (lower panel of Fig. 2). Figures 3 and 4 display the same quantities for 500-eV and for 1000-eV electrons, respectively. Note that the in-out asymmetry is enhanced for high kinetic energies. Thus, our analysis suggests that in-out asymmetries are most accentuated for high kinetic energies and for surface-crossing directions close to the surface normal, in agreement with previous studies [10].

## III. EXPERIMENT

Exposing the effect of in-out asymmetries experimentally in REEL spectroscopy is possible by comparing pairs of spectra where the position of the source and the detector is interchanged, thus interchanging the incidence and emission directions. Such pairs of scattering geometries will be called conjugate scattering geometries below. In a reflection geometry, two surface crossings occur: a first one when the probing electron enters the solid and a second one when the probing electron leaves the solid. As discussed in Sec. II, in-out differences are expected to be largest for nearly perpendicular surface crossings. Thus, in order to maximize in-out-asymmetry effects in REEL spectral features, it would appear at first glance that both the source and the detector should be aligned as close as possible to the surface normal. However, interchanging the source and the detector, if both of their angular positions lie very close to the surface normal, implies that in-out differences in the incoming segment of the trajectory effectively cancel in-out differences in the outgoing segment. In order to expose the in-out asymmetry it is therefore convenient to have one of the surface-crossing segments close to the surface normal and the other as grazing as possible. For

pairs of conjugate spectra, we therefore expect the effect of the in-out-asymmetry to be most accentuated when the angle $\theta$ between source and detector approaches 90°.

The REEL measurements presented below were carried out in an angle-resolved ADES-400 spectrometer (V.G. Scientific, UK) equipped with an EGG-3101 electron gun (Kimball Physics, Inc.), a hemispherical mirror electron energy analyzer (HMA), a dual Al/Mg x-ray source, and an EFM-3 evaporator (Omicron NanoTechnology). In order to minimize the effects of surface roughness, a thick 50-nm Al layer was evaporated *in situ* on a Si-(111) wafer at an ultrahigh-vacuum pressure of $4.1 \times 10^{-10}$ mbar and at room temperature. Indeed, atomic-force-microscopy measurements (Explorer Thermomicroscopes, USA) performed on the sample *ex situ* after completion of the measurements described below revealed a root-mean-square surface roughness of 0.8-nm height.

REEL spectra of the Al sample evaporated *in situ* were acquired at a pressure of $4.1 \times 10^{-10}$ mbar. At this pressure, x-ray photoelectron spectroscopy and Auger-electron measurements showed no traces of C or O contamination, neither before nor after the measurements. Two primary energies were considered, 500 and 1000 eV. The diameter of the electron-beam spot on the sample surface was of ~0.5 mm. The HMA was operated in fixed transmission-energy mode at a pass energy of 20 eV, leading to an energy resolution of 0.5 eV. The input aperture of the analyzer was set to a diameter of 2 mm, leading to a half-cone acceptance angle of 4.1°. Figure 5(a) depicts the scattering geometries accessible with the ADES-400 spectrometer. While the electron gun is in a fixed position, the sample can be rotated along an axis perpendicular to the page, denoted by an outgoing arrow tip with pivoting arrows, and the detector can be rotated around the sample in the detection plane, formed by the surface normal and the detection direction. By rotating the sample and the detector, one can easily access conjugate scattering geometries. The following were considered:

(i) normal incidence ($\theta_{\text{in}} = 0°$) and emission angles $\theta_{\text{out}} = \{20°, 70°, 80°\}$, Fig. 5(b), and

(ii) normal emission ($\theta_{\text{out}} = 0°$) and incidence angles $\theta_{\text{in}} = \{20°, 70°, 80°\}$, Figs. 5(c)–5(e).

For angle-resolved measurements the electron-beam spot on the sample surface must coincide with the center of rotation of the HMA. The position of the electron-beam spot on the sample was carefully aligned with the center of rotation of the HMA using a laser-beam alignment technique. The alignment was carried out separately for normal-incidence and normal-emission geometry. During measurements with normal incidence and varying emission angles, Fig. 5(b), the sample position (and therefore the electron-beam spot on the sample as well) is fixed and thus the alignment performed for one emission angle is preserved for all emission angles. During measurements with normal emission, Figs. 5(c)–5(e), the sample is rotated. In these cases, the position of the electron-beam spot on the sample was rechecked with the aforementioned laser technique for each considered incidence angle.

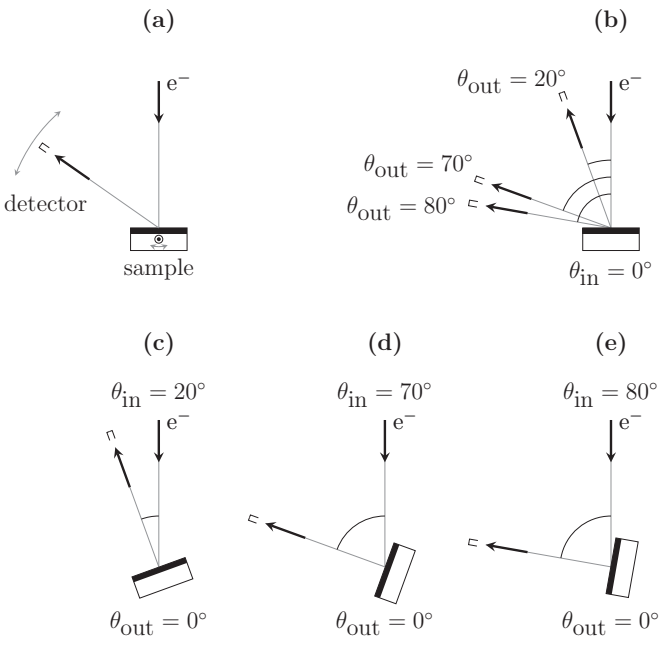


FIG. 5. (a) Angular degrees of freedom of the ADES-400 spectrometer; both the sample and the detector can be rotated in the detection plane. (b) Scattering geometries considered in normal-incidence measurements. (c)–(e) Scattering geometries considered in normal-emission measurements, corresponding to the conjugate geometries in normal-incidence mode.

## IV. RESULTS AND DISCUSSION

The experimental spectra are displayed in Fig. 6, grouped in pairs corresponding to conjugate scattering geometries. Red solid curves represent spectra for normal incidence (i), whereas blue dashed curves represent spectra for normal emission (ii); the angle $\theta$ is the angle between source and detector. Apart from the single-scattering surface (energy loss $\Delta E = 10.4$ eV, 1s) and bulk ($\Delta E = 15.3$ eV, 1b) plasmon, multiple excitation of plasmons can be discerned at 20.8 eV (2s), 25.7 eV (1b1s), and 30.6 eV (2b). The spectra were normalized to the height of the elastic peak. For bulk losses, which are independent of position and of direction of motion for a polycrystalline material, this normalization merely accounts for the fact that, for a fixed primary energy, conjugate scattering geometries lead to different backscattering probabilities [17]. Indeed, after normalization, all conjugate REEL spectra are virtually identical, with the exception of the surface plasmon peak, which exhibits marked differences that increase with the angle between the source and detector, as anticipated above. The fact that these differences appear only for surface losses supports the reliability of the experimental procedure and allows us to interpret the different intensities in the surface-loss peaks as a direct signature of the in-out asymmetry in surface excitations. Indeed, the magnitude of this asymmetry increases as the angle between source and analyzer increases ($\theta \to 90°$), i.e., as a scattering geometry is attained where one of the in/out segments is grazing and the other is parallel to the surface normal ($\eta \to 0°$), as anticipated above.

The experimental spectra follow roughly the anticipated energy behavior: for single perpendicular surface crossings

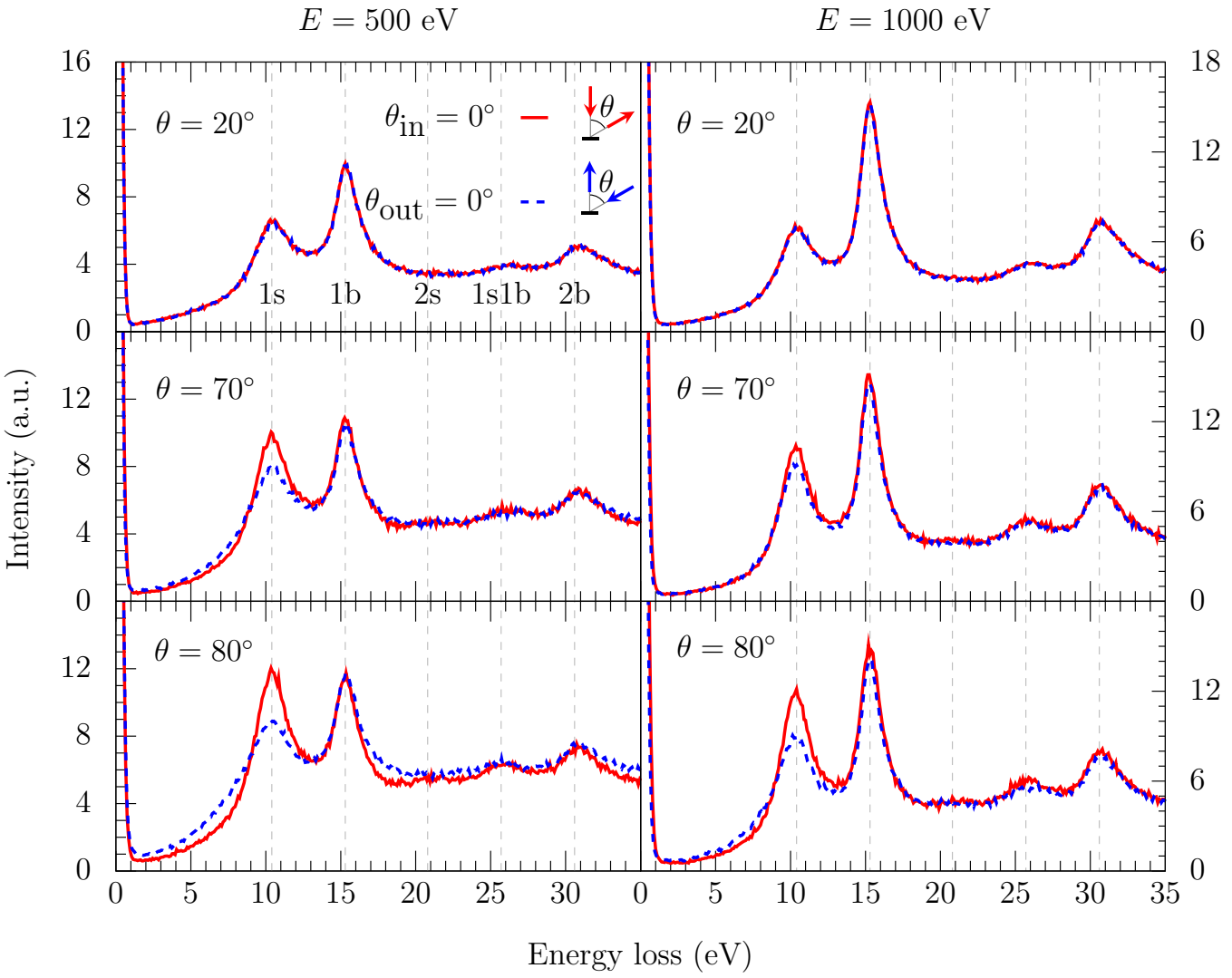


FIG. 6. (Color online) Pairs of conjugate REEL spectra of Al measured with a primary energy of 500 eV (left) and 1000 eV (right), normalized to the height of the elastic peak. Apart from the single-scattering surface (energy loss $\Delta E = 10.4$ eV, 1s) and bulk ($\Delta E = 15.3$ eV, 1b) plasmon, multiple excitation of plasmons can be discerned at 20.8 eV (2s), 25.7 eV (1b1s), and 30.6 eV (2b). Red solid (blue dashed) curves correspond to spectra with normal incidence (emission). The angle $\theta$ is the angle between the source and the detector.

(lower two panels of Fig. 6), the net area difference between surface features in spectra corresponding to incoming and outgoing normal segments is larger for 1000 eV than for 500 eV. Finally, we note that the in-out-asymmetry effect is by no means negligible: it amounts to experimentally observed differences of up to 30% in the intensity of the surface-plasmon peak in conjugate pairs of REEL spectra of Al. Thus, any model used for a quantitative interpretation of REEL spectra should capture the in-out asymmetry effect. Finally, we note that for large angles between source and analyzer (lower panels in Fig. 6) the low-energy-loss domain appears broader. This effect seems to affect predominantly the surface-loss features and therefore does not affect the present discussion on the magnitude of in-out differences.

The energy- and angular-dependence exhibited by the in-out asymmetry can be qualitatively understood as follows. In the case of perpendicular trajectories, the induced electric field has a single component along the direction of motion. Thus, all in-out asymmetries translate directly into the induced electric field and therefore into the surface-stopping characteristics of the projectile. For oblique trajectories, the induced electric field has an additional component perpendicular to the direction of motion (which does no work on the projectile). Thus, in-out asymmetries no longer affect a single component of the stopping force, but distribute into the two components of the induced electric field, resulting in the observed diminishing of the in-out asymmetry.

The following counterintuitive fact is worthwhile noting. Whereas the probability for surface excitations is proportional to [18] $1/(\sqrt{E}\cos\eta)$, i.e., proportional to the surface-crossing time to a first approximation [19], the importance of in-out-asymmetry effects scales inversely: it is accentuated for high energies and surface-crossing directions close to the surface normal. Thus, the indicators we have given above to estimate the importance of the in-out-asymmetry effect should be taken as approximate guidelines.

## V. CONCLUSIONS

We have presented a series of REEL spectra of polycrystalline Al, which exhibit an in-out asymmetry in the surface energy-loss characteristics. The effect is qualitatively understood on the basis of the semiclassical dielectric formalism after a systematic study of the energy- and angle-dependence of the stopping power in the very vicinity of the interface, focusing on differences between incoming and outgoing trajectories. A minor mathematical simplification has been made to somewhat alleviate the calculation, resulting in a slight distortion of the energy and intensity of surface modes, but nevertheless retaining the essential energy- and angular dependence required for the present qualitative analysis. We verify and justify the known fact that in-out asymmetries are enhanced for surface-crossing angles close to the surface normal and (overall) for increasing energies. The experimental data are in good agreement with the expected behavior and constitute a clear signature of the in-out asymmetry in surface excitations. These asymmetries amount to differences of up to 30% in the intensity of surface energy-loss features in REEL spectra.

## ACKNOWLEDGMENTS

F.S.-P. gratefully acknowledges the support of the Alexander von Humboldt Foundation through a Humboldt Research Fellowship. This work was carried out in the framework of Project No. P20891-N20, funded by the Austrian "Fonds zur Förderung der wissenschaftlichen Forschung." Support by the Academy of Sciences of the Czech Republic (P.J. and J.Z.) through Project No. M100101202 is highly appreciated. The computational results presented here have been achieved in part using the Vienna Scientific Cluster (VSC). We thank Prof. J. Burgdörfer and Prof. F. Salvat for fruitful discussions.

[1] T. L. Kirk, U. Ramsperger, and D. Pescia, J. Vac. Sci. Technol. B **27**, 152 (2009).
[2] T. L. Kirk, O. Scholder, L. G. De Pietro, U. Ramsperger, and D. Pescia, Appl. Phys. Lett. **94**, 153502 (2009).
[3] I. Utke, P. Hoffmann, and J. Melngailis, J. Vac. Sci. Technol. B **26**, 1197 (2008).
[4] M. Huth, F. Porrati, C. Schwalb, M. Winhold, R. sachser, M. Dukic, J. Adams, and G. Fantner, Beilstein J. Nano. **3**, 597 (2012).
[5] F. Porrati, R. Sachser, C. H. Schwalb, A. S. Frangakis, and M. Huth, J. Appl. Phys. **109**, 063715 (2011).
[6] S. Mehendale, J. J. L. Mulders, and P. H. F. Trompenaars, Nano **24**, 145303 (2013).
[7] F. Yubero, J. M. Sanz, B. Ramskov, and S. Tougaard, Phys. Rev. B **53**, 9719 (1996).
[8] Z.-J. Ding, J. Phys.: Condens. Mat. **10**, 1733 (1998).
[9] B. Da, S. F. Mao, and Z. J. Ding, J. Phys.: Condens. Mat. **23**, 395003 (2011).
[10] F. Salvat-Pujol and W. S. M. Werner, Surf. Interface Anal. **45**, 873 (2013).
[11] J. L. Gervasoni, R. O. Barrachina, and W. S. M. Werner, Surf. Interface Anal. **45**, 1849 (2013).
[12] Z.-J. Ding, J. Phys.-Condens. Mat. **10**, 1753 (1998).
[13] Y. C. Li, Y. H. Tu, C. M. Kwei, and C. J. Tung, Surf. Sci. **589**, 67 (2005).
[14] W. S. M. Werner, W. Smekal, T. Cabela, C. Eisenmenger-Sittner, and H. Störi, J. Electron Spectrosc. Relat. Phen. **114–116**, 363 (2001).
[15] F. Salvat-Pujol, Ph.D. thesis, Technische Universität Wien (2012).
[16] W. S. M. Werner, F. Salvat-Pujol, A. Bellissimo, R. Khalid, W. Smekal, M. Novak, A. Ruocco, and G. Stefani, Phys. Rev. B **88**, 201407(R) (2013).
[17] F. Salvat-Pujol and W. S. M. Werner, Phys. Rev. B **83**, 195416 (2011).
[18] W. S. M. Werner, W. Smekal, F. Salvat-Pujol, Z. Halavani, S. Pfleger, J. Rastl, and C. Eisenmenger-Sittner, Appl. Phys. Lett. **98**, 193111 (2011).
[19] W. S. M. Werner, M. Novak, F. Salvat-Pujol, J. Zemek, and P. Jiricek, Phys. Rev. Lett. **110**, 086110 (2013).